

AD-A263 127



OFFICE OF NAVAL RESEARCH

Grant N00014-93-1-0351

R & T Code 4133020 - - -09

Technical Report No. 5

DTIC  
ELECTE  
APR 21 1993  
S C D

2

Adsorption Study of Cysteine, N-acetylcysteamine, Cysteinesulfinic Acid and Cysteic Acid on a  
Polycrystalline Gold Electrode

by

W. Ronald Fawcett, Milan Fedurco, Zuzana Kováčová and Zofia Borkowska

Prepared for Publication

in

Journal of Electroanalytical Chemistry

Department of Chemistry  
University of California  
Davis, CA 95616

April 15, 1993

Reproduction in whole or in part is permitted  
for any purpose of the United States Government

"This document has been approved for public release  
and sale; its distribution is unlimited"

88 4 20 060

93-08420



28p8

## REPORT DOCUMENTATION PAGE

1. AGENCY USE ONLY (Leave blank)		2. REPORT DATE April 15, 1993	3. REPORT TYPE AND DATES COVERED Technical
4. TITLE AND SUBTITLE Adsorption Study of Cysteine, N-acetylcysteamine, Cysteinesulfinic Acid and Cysteic Acid on a Polycrystalline Gold Electrode		N00014-93-1-0351	
6. AUTHOR(S) W. Ronald Fawcett, Milan Fedurco, Zuzana Kovacova and Zofia Borkowska			
7. PERFORMING ORGANIZATION NAME(S) AND ADDRESS(ES) Department of Chemistry University of California Davis, CA 95616		8. PERFORMING ORGANIZATION REPORT NUMBER  No. 5	
9. SPONSORING/MONITORING AGENCY NAME(S) AND ADDRESS(ES) Office of Naval Research 800 N. Quincy Arlington, VA 22217-5000		10. SPONSORING/MONITORING AGENCY REPORT NUMBER	
11. SUPPLEMENTARY NOTES Prepared for publication in Journal of Electroanalytical Chemistry			
12a. DISTRIBUTION/AVAILABILITY STATEMENT  Unclassified		12b. DISTRIBUTION CODE	
13. ABSTRACT (Maximum 200 words)  Capacity against potential data for the adsorption of cysteine and other organosulfur compounds on polycrystalline gold are reported. Cysteine, N-acetylcysteamine and cysteinesulfinic acid form monolayers on gold through the thiol group, and significantly lower the interfacial capacity in the double layer region. On the other hand, cysteic acid forms multilayers under the same conditions. The surface excess of the compounds at full monolayer coverage has been estimated, and compared with the data for the adsorption of simple n-alkylthiols. It is argued that the packing of the cysteine and related compounds is more compact due to strong electrostatic interactions.			
14. SUBJECT TERMS		15. NUMBER OF PAGES	
		16. PRICE CODE	
17. SECURITY CLASSIFICATION OF REPORT  Unclassified	18. SECURITY CLASSIFICATION OF THIS PAGE  Unclassified	19. SECURITY CLASSIFICATION OF ABSTRACT  Unclassified	20. LIMITATION OF ABSTRACT  Unclassified

**Adsorption Study of Cysteine, N-acetylcysteamine,  
Cysteinesulfinic Acid and Cysteic Acid  
on a Polycrystalline Gold Electrode**

W. Ronald Fawcett, Milan Fedurco, Zuzana Kováčová  
and Zofia Borkowska

Department of Chemistry  
University of California  
Davis, CA 95616

**ABSTRACT**

Capacity against potential data for the adsorption of cysteine and other organosulfur compounds on polycrystalline gold are reported. Cysteine, N-acetylcysteamine and cysteinesulfinic acid form monolayers on gold through the thiol group, and significantly lower the interfacial capacity in the double layer region. On the other hand, cysteic acid forms multilayers under the same conditions. The surface excess of the compounds at full monolayer coverage has been estimated, and compared with the data for the adsorption of simple n-alkylthiols. It is argued that the packing of the cysteine and related compounds is more compact due to strong electrostatic interactions.

Accession For	
NTIS	CRA&I <input checked="" type="checkbox"/>
DTIC	TAB <input type="checkbox"/>
Unannounced <input type="checkbox"/>	
Justification	
By	
Distribution /	
Availability Codes	
Dist	Avail and/or Special
A-1	

## INTRODUCTION

The importance of intermolecular interactions in determining the structure of hydrophobic films of alkylthiols and dialkyl sulfides on gold has been considered both with respect to the length of the alkyl chain and nature of the headgroup [1]. The simple water soluble organosulfur compound, cysteine, forms thin films on gold in aqueous solutions [2,3] but the nature of intermolecular interactions are expected to be quite different. This follows from the fact that cysteine has a zwitterionic structure so that strong electrostatic interactions are important in determining molecular packing at the electrode/solution interface. In addition considerable interest has been shown in the potential application of chemisorbed cysteine derivatives as electron transfer "promoters" [4] and for immobilization of electroactive species on solid electrodes [5]. We have recently carried out a study of the electrocatalytic oxidation of cysteine (RSH) and the related compounds cysteinesulfinic acid (RSO<sub>2</sub>H) and cysteic acid (RSO<sub>3</sub>H) on a polycrystalline gold [6]. It was clear from this work that considerable change in interfacial properties in the double layer occurred in the presence of these compounds. In the present paper we report a study of the effect of these water soluble compounds on double layer properties using the a.c. admittance technique [7]. The study was extended to include

a more hydrophobic molecule N-acetylcysteamine in order to assess in a preliminary manner the effect of alkyl chain length on the changes in double layer properties.

## EXPERIMENTAL

### Apparatus

Cyclic voltammograms were obtained using the apparatus described in the previous paper [6]. In the case of a.c. admittance measurements, the linear potential ramp and sinusoidal perturbation (10 mV peak-to-peak) were provided by a Solartron 1250 frequency response analyzer. This signal was fed into the external input of an EG&G PAR 175 potentiostat. The output of the current follower EG&G PAR 176 and the reference signal from the potentiostat PAR 175 were fed into two channels of the same Solartron analyzer to obtain the in- and out-of-phase components of admittance. The input of all parameters for a.c. voltammetric measurements and data acquisition control were performed by a dedicated IBM microcomputer through a DAS 16 interface board. The phase shift connected with other elements of the circuit was corrected using a dummy cell consisting of a resistance and capacitance in a range appropriate for the real system.

Measurements were conducted in a three electrode cell with working, reference and counter electrode as previously

described [6]. All potentials are reported with respect to a calomel electrode containing 0.05 M KCl.

### Chemicals

All chemical reagents used in the present work were those described earlier [6] except for the N-acetylcysteamine (97% pure, Aldrich). Its solutions were prepared fresh by dilution of aliquot amounts of the compound in ultrapure water. The procedures including the water purification, the glass cleaning and the transfer experiment were identical to those described earlier [6].

### Measurements and data analysis

Admittance data were collected at six frequencies (25-250 Hz) in order to correct for anticipated frequency dispersion [7], and in the potential range from -0.5 to 0.6 V at 50 mV increments, if not stated otherwise. Data collection at each potential required 42 s and included three sets of values at each frequency. Specific capacity,  $C$ , was estimated on the basis of the constant phase element model (CPE) [8], according to which the impedance is given by

$$Z = R_s + R_s^{1-n} / (j\omega C)^n \quad (1)$$

where  $R_s$  is the cell resistance,  $\omega$ , the angular frequency and  $n$ , a dimensionless parameter close to unity.

The logarithm of the out-of-phase impedance is then [8]<sup>\*</sup>

$$\ln Z_I = \ln \cos[(1-n)\pi/2] - n \ln \omega C + (1-n) \ln R_S \quad (2).$$

Accordingly, the parameter  $n$  can be determined from of a plot of  $\ln Z_I$  against  $\ln(\text{frequency})$ . The cell resistance was found from the intercept of a plot of real component of the impedance,  $Z_R$ , against  $Z_I$ . Values of the parameter  $n$  were determined in the whole potential range studied in order to assess changes in the degree to which the system departs from the simple Randles model of the interface.

---

\* It should be noted that equation (5) in reference [7] is incorrectly written with the logarithm of the real component  $Z_R$  on the left hand side. It should be the same as equation (2) above. However, Figure 5 in this paper correctly shows a plot of  $\ln Z_I$  against the logarithm of frequency as the means of determining the parameter  $n$ .

---

## RESULTS AND DISCUSSION

### Capacity data in HClO<sub>4</sub> solutions

Capacity-potential curves for the polycrystalline gold electrode/aqueous solution interface with 0.01 M HClO<sub>4</sub> as electrolyte obtained from three independent measurements in the time span of one month are shown in Figure 1. The excellent reproducibility of the data confirms that the

level of impurities at the electrode/solution interface and the real surface area do not change significantly after a relatively long period of time. The cell resistance measured in 0.01 M  $\text{HClO}_4$  was in the range 600-800  $\Omega$ . The parameter  $n$  varied from 0.95 to 0.99 in the potential region from -0.5 to +0.6 V. According to the Gouy-Chapman model, the minimum on the capacity curve in the absence of adsorption of ions in a supporting electrolyte of low ionic strength corresponds to the potential of zero charge (p.z.c.). On the basis of the present results, the p.z.c. for a polycrystalline gold electrode in 0.01 M  $\text{HClO}_4$  is  $-0.200 \pm 0.005$  V against the calomel electrode.

The most common contaminants in electrochemical experiments on gold electrodes are reported to be anionic species such as chlorides and sulphates, which specifically adsorb on gold at positive charge densities [9]. Their presence at the electrode surface can be recognized from the capacity data since the adsorption of halides tends to increase capacity values at positive charge densities. It is our experience that the blocking effect of halide anions and organic contaminants on the adsorption of water or hydroxyl ions results in very similar cyclic voltammetric curves for the potential region where gold oxidation takes place. On the other hand, organic contaminants cause a pronounced decrease in capacity values, usually around the more positive maximum of the capacity curve. No significant effect of stirring on the shape of the curves was observed



in the double layer region. Convection would eventually increase the flux of contaminants towards the electrode and their subsequent adsorption at the electrode/solution interface. Outside of the double layer region, no significant change in the current of the peak corresponding to the deposition of hydroxyl ions was observed after completing the a.c. admittance measurement (16 minutes) while stirring the solution in the potential range from -0.5 to +0.6 V. These observations further confirm that the level of anionic contaminants in 0.01 M  $\text{HClO}_4$  is low and that the presence of organic impurities in the polarographic cell can be avoided by careful glass cleaning procedures [6].

#### **cysteine adsorption on the gold electrode**

The amino acid cysteine is a small but highly polar molecule. Depending on pH, all of its functional groups can be ionized ( $\text{pK}_a$  values: 1.92, 8.35 and 10.46) [10]. Therefore it does not behave as a simple dipole. Its orientation in the electric field of the polarizable electrode/solution interface depends on the magnitude and the location of the charge within the molecule. Another complication arises from the fact that  $\text{RSH}$  irreversibly reacts with gold forming a monovalent surface compound. Nuzzo et al. [11] have estimated the strength of the gold-sulfur bond in a simple organic thiolate, such as gold

methanethiolate, to be  $188 \text{ kJ mol}^{-1}$ . The large energy of chemical bond formation between cysteine and Au is responsible for the irreversible adsorption of the molecule in spite of its good solubility in water.

The potential of the polarizable electrode at open circuit was found to be  $+ 0.020 \text{ V}$  against the calomel electrode, that is,  $220 \text{ mV}$  more positive than the p.z.c.. Therefore all double layer experiments had to be carefully designed so that this electrode came into contact with the solution of RSH at an applied potential of  $-0.500 \text{ V}$  at the start of experiment. Capacity data for a very dilute solution of RSH ( $1.2 \mu\text{M}$ ) recorded with different data acquisition patterns are shown in Figure 2 for d.c. potentials from  $-0.5$  to  $0.6 \text{ V}$ . In spite of the fact that the solution was stirred, the equilibrium value of the capacity, especially at negative potentials, was not reached during the time that data were collected. However, these non-equilibrium results are of interest because they show the changes occurring at the interface as cysteine replaces water molecules. From these experiments, especially when carried out at lower cysteine concentrations, it is clear that the p.z.c. shifts slightly to more positive potentials with adsorption. The capacity maximum at negative potentials shifts to more positive potentials, then back in the negative direction and eventually disappears in the potential range considered. The capacity maximum at positive potentials observed in the absence of adsorption is

suppressed in its presence. Furthermore, the onset of gold oxidation due to adsorption of water seen at potentials more positive than 0.45 V is completely suppressed when cysteine is adsorbed. This behaviour persists up to +0.7 V where the chemisorbed cysteine is itself oxidized. At equilibrium, the capacity curve is rather featureless with a shallow minimum in the polarizable range, that is from the potential at which hydrogen evolution begins to the potential at which cysteine oxidation is observed.

Effects related to the time taken to achieve full coverage can also be seen from cyclic voltammetric experiments (Fig. 3). The electrode was exposed to 1.2  $\mu\text{M}$  cysteine at -0.5 V for 10 minutes, and then a cyclic voltammogram recorded. Integration of the oxidation current resulting from a complete cysteine monolayer results in a charge  $Q_a$  (curve a in Fig. 3). The potential sweep was continued with resulting desorption of the oxidation product and reduction of gold oxide at 0.65 V; then the sweep was reversed at -0.5 V and a second oxidation sweep performed without interruption (curve b in Fig. 3). The resulting charge  $Q_b$  is less than that resulting from oxidation of a monolayer because the bulk concentration of cysteine was not sufficiently high to form a monolayer during the sweep period of the cyclic voltammetric experiment. The charge  $Q_b$  does not change with further cycling and corresponds to the steady state coverage for the given bulk concentration of RSH and sweep rate.

Neither the pzc nor the charge density at the gold electrode/solution interface could be determined from a.c. admittance data since the capacity curves a-e in Fig. 2 do not correspond to equilibrium data. Therefore, surface coverage cannot be estimated from the relative decrease in capacity with cysteine concentration at constant potential. The dependence of capacity on time in the double layer region was also studied. On the basis of data presented in Fig. 4 it was concluded that the capacity is approximately independent of potential in this range. Full surface coverage is obtained by the adsorption of cysteine from 1.2  $\mu$ M RSH at any potential in the same time (10 minutes) and all experimental points can be fitted with a single curve.

#### **Adsorption of other organosulfur compounds on the gold electrode**

The general features of the capacity curves in the presence of cysteinesulfinic acid (Fig. 5) are similar those obtained for cysteine. Again, with increase in the bulk concentration of this compound there is a decrease in capacity values at potentials negative of -0.35 V. Since  $\text{RSO}_2\text{H}$  is an acid, and some of its  $-\text{SO}_2\text{H}$  groups are dissociated in 0.01 M  $\text{HClO}_4$  ( $\text{pK}_a$  for  $-\text{SO}_2\text{H}$  is 2.1) [10], one might to expect it to behave differently. By transferring the gold electrode from  $\text{RSO}_2\text{H}$  solutions to another cell containing only 0.01 M  $\text{HClO}_4$ , it was confirmed that  $\text{RSO}_2\text{H}$  is

chemisorbed on the gold electrode surface and that the adsorption process is potential independent. The resulting equilibrium curve is rather featureless with a minimum capacity that is slightly higher than that observed in the presence of cysteine (Fig. 5).

Another compound studied was N-acetylcysteamine. It behaved similarly to cysteine as one would expect since both molecules have the same surface active thiol group. However, N-acetylcysteamine is more hydrophobic because of its longer alkyl chain. The interfacial capacity for this system at equilibrium (Figure 5, curve c) is similar to that for cysteine but with a lower capacity over most of the polarizable range of the electrode. This observation undoubtedly reflects the fact that the inner layer is thicker in the presence of this adsorbate.

Capacity curves illustrating cysteic acid adsorption on gold are shown in Fig. 6. This system is quite different than the others studied, causing a large increase in capacity at potentials positive of the p.z.c.. No significant adsorption of this compound could be detected at negative potentials for a large range of bulk concentrations (6 orders of magnitude). It should also be emphasized that the data presented at positive potentials are not equilibrium data, further increase in capacity being observed with time. The present data can be compared with those reported earlier by Silva et al. [12] for the adsorption of sulphamic acid on gold single crystals.

Although a qualitatively similar capacity peak was found in the case of sulphamic acid, this compound is not oxidized at more positive potentials, whereas cysteic acid is. The capacity features for the present system are attributed to multilayer formation as suggested by the earlier cyclic voltammetric data [6]. Both cysteic acid and sulphamic acid are adsorbed on Au through the  $\text{-SO}_3^-$  group. However, cysteic acid has the electropositive  $\text{-NH}_3^+$  group at the other end of the molecule; this can electrostatically interact with the  $\text{-SO}_3^-$  group on another molecule with the result that multilayers of adsorbate are formed. As shown earlier [6], the subsequent layers of cysteic acid can be removed by washing whereas the first chemisorbed layer can only be removed by oxidative desorption.

#### **Molecular properties of adsorbate film**

In the previous paper [6], the method of assessing coverage of the gold electrode by water soluble organosulfur compounds using cyclic voltammetry was described. The surface excess was estimated from the charge associated with oxidative desorption of an adsorbate monolayer after transferring the modified gold electrode to another cell containing just the electrolyte (0.01 M  $\text{HClO}_4$ ). The relationship between the surface excess  $\Gamma$  and the charge associated with oxidative desorption  $Q$  is

$$\Gamma = Q/n_eFA \quad (2)$$

where  $n_e$  is the number of electrons associated with the oxidation reaction and  $A$ , the electrode area, and  $F$ , the Faraday. Values of  $\Gamma$ ,  $Q$ ,  $n_e$ , and the area per molecule in the monolayer are summarized for the four compounds in Table 1.

The estimated area per molecule in the monolayer is quite small for the systems studied, namely less than  $0.1 \text{ nm}^2 \text{ molecule}^{-1}$ . The charge associated with oxidation of a cysteine monolayer is considerably larger than that found for oxidation of *n*-alkylthiols on gold ( $280 \mu\text{C cm}^{-2}$  for  $3 < n < 18$ ) [13]. The projected geometric area for *n*-decanethiol chemisorbed on gold has been estimated to be  $0.184 \text{ nm}^2$  [14]. It follows that the packing of cysteine is much more efficient, probably because of strong electrostatic interactions between the molecule in the monolayer. X-Ray photoelectron spectroscopic studies of cysteine deposited under UHV conditions at  $-50^\circ\text{C}$  have shown that cysteine forms multilayers on gold about  $4.0 \text{ nm}$  thick [3]. The same authors proposed a hydrogen-bonded zwitterionic bilayer structure, with an average film thickness of  $0.6 \text{ nm}$ , after the self-assembly of cysteine from its  $1.0 \text{ mM}$  solution in water (pH 1.5). From a model for the cysteine molecule constructed on the basis of crystallographic bond lengths and bond angles [15] (Figure 7), the thickness of a cysteine monolayer should be about  $0.6 \text{ nm}$  at the packing density determined in this study. It

is interesting that the number of surface gold atoms on a polycrystalline gold electrode, calculated from the charge necessary to form a monolayer of gold oxide [16] agrees approximately with a number of sulfur atoms per unit area chemisorbed on the same substrate. This indicates that the bilayer structure in which one cysteine molecule adsorbed through its sulfur atom and adjacent one with its thiol group pointing away from the metal [3] is improbable; such a configuration would result in a smaller charge for cysteine oxidation than experimentally measured here. As shown in Table 1, the area occupied by the RSH and RSO<sub>2</sub>H molecules is similar but differs from that for RSO<sub>3</sub>H. Repulsion between the dissociated sulfonic group of cysteic acid molecules at the electrode/solution interface might influence its surface coverage. N-acetylcysteamine gives values of capacity at maximum surface coverage which are lower by approximately  $7.0 \mu\text{F cm}^{-2}$  than RSH in spite of the fact that the surface coverage by this molecule is lower than that of cysteine (see Table 1). This result is attributed to a thicker monolayer film in the presence of N-acetylcysteamine. The degree in ordering of N-acetylcysteamine films is smaller than in the case of cysteine but significantly differs from that of short chain n-alkylthiols ( $n < 7$ ). The latter are more desorganized compared to N-acetylcysteamine on the basis of spectroscopic and ellipsometric studies [17].



## CONCLUSIONS

Cysteine, cysteinesulfinic acid and cysteic acid form a group of water soluble compounds where the molecule moiety  $\text{HOOC-CH}(-\text{NH}_2)\text{-CH}_2\text{-}$  remains unchanged, whereas the sulfur atom undergoes gradual oxidation. The present adsorption studies have shown that intermolecular interactions between the chemisorbed molecules control the degree of ordering and packing density of these compounds on the gold electrode surface. It is probable that electrostatic forces between ionized carboxylic and amine groups of neighbouring cysteine molecules cause a significant hindrance in the rotation of molecule around the axis vertical to the electrode surface. In addition, the rotation of  $-\text{NH}_3^+$  and  $-\text{COO}^-$  groups bonded to the C5 carbon (see Fig. 7) creates a cavity for the functional group of the opposite charge. *This energetically favourable geometry effectively increases packing density of cysteine at the electrode surface.* Films of N-acetyl-cysteamine are more hydrophobic than those of cysteine and the degree of their ordering is controlled through weaker van der Waals forces. Since this molecule contains no carboxylic group and the  $-\text{NH}_2$  group is blocked by the  $-\text{CO-CH}_3$  group, its rotation at maximum surface coverage is not electrostatically "frozen". The thermal motion of chemisorbed N-acetylcysteamine results in a smaller surface coverage than in the case of cysteine. The present work demonstrates that the adsorption parameters for water soluble sulfur compounds can be obtained with good

reproducibility on a clean gold electrode surface. The a.c. admittance technique appears to be very promising for qualitatively characterizing thiol films; moreover, surface coverage data for the adsorbates can be extracted from cyclic voltammetric data obtained in the potential region where adsorbate oxidation occurs.

#### ACKNOWLEDGEMENT

The financial support of the Office of Naval Research, Washington is gratefully acknowledged.

#### REFERENCES

1. E.B. Troughton, C.D. Bain, G.M. Whitesides, R.G. Nuzzo, D.L. Allara and M.D. Porter, *Langmuir*, 4 (1988) 365.
2. A. Ihs and B. Liedberg, *J. Colloid Interface Sci.*, 144 (1991) 282.
3. K. Uvdal, P. Bodo and B. Liedberg, *J. Colloid Interface Sci.*, 149 (1992) 162.
4. P.D. Barker, H.A.O. Hill and N.J. Walton, *J. Electroanal. Chem.*, 260 (1989) 303.
5. E.Y. Katz and A.A. Solove'v, *J. Electroanal. Chem.*, 291 (1990) 171.
6. W.R. Fawcett, M. Fedurco, Z. Kováčová and Z. Borkowska, *J. Electroanal. Chem.*, submitted.
7. W.R. Fawcett, Z. Kováčová, A.J. Motheo and C.A. Foss, Jr., *J. Electroanal. Chem.*, 326 (1992) 91.
8. G.J. Brug, A.L.G. van den Eeden, M. Sluyters-Rehbach

- and J.H. Sluyters, *J. Electroanal. Chem.*, 176 (1984) 275.
9. A. Hamelin in B.E. Conway, R.E. White and J.O'M. Bockris (Eds.), *Modern Aspects of Electrochemistry*, No. 16, Plenum Press, New York (1985) Ch. 1.
  10. G.D. Fasman, *Practical Handbook of Biochemistry and Molecular Biology*, CRC Press, Boca Raton (1990) pp. 3-68.
  11. R.G. Nuzzo, B.R. Zegarski and L.H. Dubois, *J. Am. Chem. Soc.*, 109 (1987) 733.
  12. F. Silva, C. Moura and A. Hamelin, *Electrochim. Acta*, 34 (1989) 1665.
  13. C.A. Widrig, C. Chung and M.D. Porter, *J. Electroanal. Chem.*, 310 (1991) 335.
  14. C.E.D. Chidsey and D.L. Loiacono, *Langmuir*, 6 (1990) 682.
  15. M.M. Harding and H.A. Long, *Acta Crystallogr., Sect. B*, 24 (1968) 1096.
  16. H. Angerstein-Kozłowska, B.E. Conway, A. Hamelin and L. Stoicoviciu, *Electrochim. Acta*, 31 (1986) 1051.
  17. M.D. Porter, T.B. Bright, D.L. Allara and C.E.D. Chidsey, *J. Am. Chem. Soc.*, 109 (1987) 3559.

Table 1

Monolayer oxidation	RSH	RSO <sub>2</sub> H	RSO <sub>3</sub> H	N-acetylcysteamine
Number of electrons, $n_e$	4	2	1	4
Charge, Q, $\mu\text{C cm}^{-2}$	900	450	200	650
Surface concentration, $\Gamma$ , moles $\text{cm}^{-2} \times 10^9$	2.3	2.3	2.1	1.7
Area per molecule $\text{nm}^2$	0.071	0.071	0.080	0.098

### Legends for Figures

**Figure 1** Experimental interfacial capacity data for a polycrystalline gold electrode in 0.01 M  $\text{HClO}_4$  against electrode potential. The data were obtained from three independent measurements in the time span of one month.

**Figure 2** Capacity against electrode potential at a Au electrode in 0.01 M  $\text{HClO}_4$  with 1.2  $\mu\text{M}$  cysteine recorded with varying times at each potential : a) 42 s at each potential; 50 mV steps; b) 84 s at each potential; 50 mV steps; c) 126 s at each potential; 50 mV steps; d) 126 s at each potential; 25 mV steps; e) 126 s at each potential; 5 mV steps. Curve f gives the capacity in the absence of cysteine.

**Figure 3** Cyclic voltammograms at the gold electrode recorded in 0.01 M  $\text{HClO}_4$  with 1.2  $\mu\text{M}$  cysteine after holding the electrode at -0.5 V for 10 minutes. Curve a corresponds to the first sweep during which a full monolayer of cysteine is oxidized and curve b shows the result of subsequent sweeps. Scan rate: 20  $\text{mV s}^{-1}$ .

**Figure 4** Specific capacity at the gold electrode in 0.01 M  $\text{HClO}_4$  with 1.2  $\mu\text{M}$  cysteine at fixed potential as a function of time. The potentials are -0.4 V (○), -0.3 V (●), -0.2 V (Δ) and -0.1 V (▲).

**Figure 5** Plots of the specific capacity at the gold electrode against electrode potential in 0.01 M  $\text{HClO}_4$  in the presence of N-acetylcysteamine (a), cysteine (b), and cysteinesulfinic acid (c) under conditions that the full surface coverage is achieved. Curves d gives the capacity in the absence of cysteine.

**Figure 6** Capacity against electrode potential curves at a Au electrode in 0.01 M  $\text{HClO}_4$  with varying amounts of cysteic acid: a) 10, b) 100 and c) 1000  $\mu\text{M}$ . The curves were recorded at 50 mV intervals with 42 s at each potential. Curve d gives the capacity in the absence of cysteic acid.

**Figure 7** Crystallographic structure of L-cysteine [15].

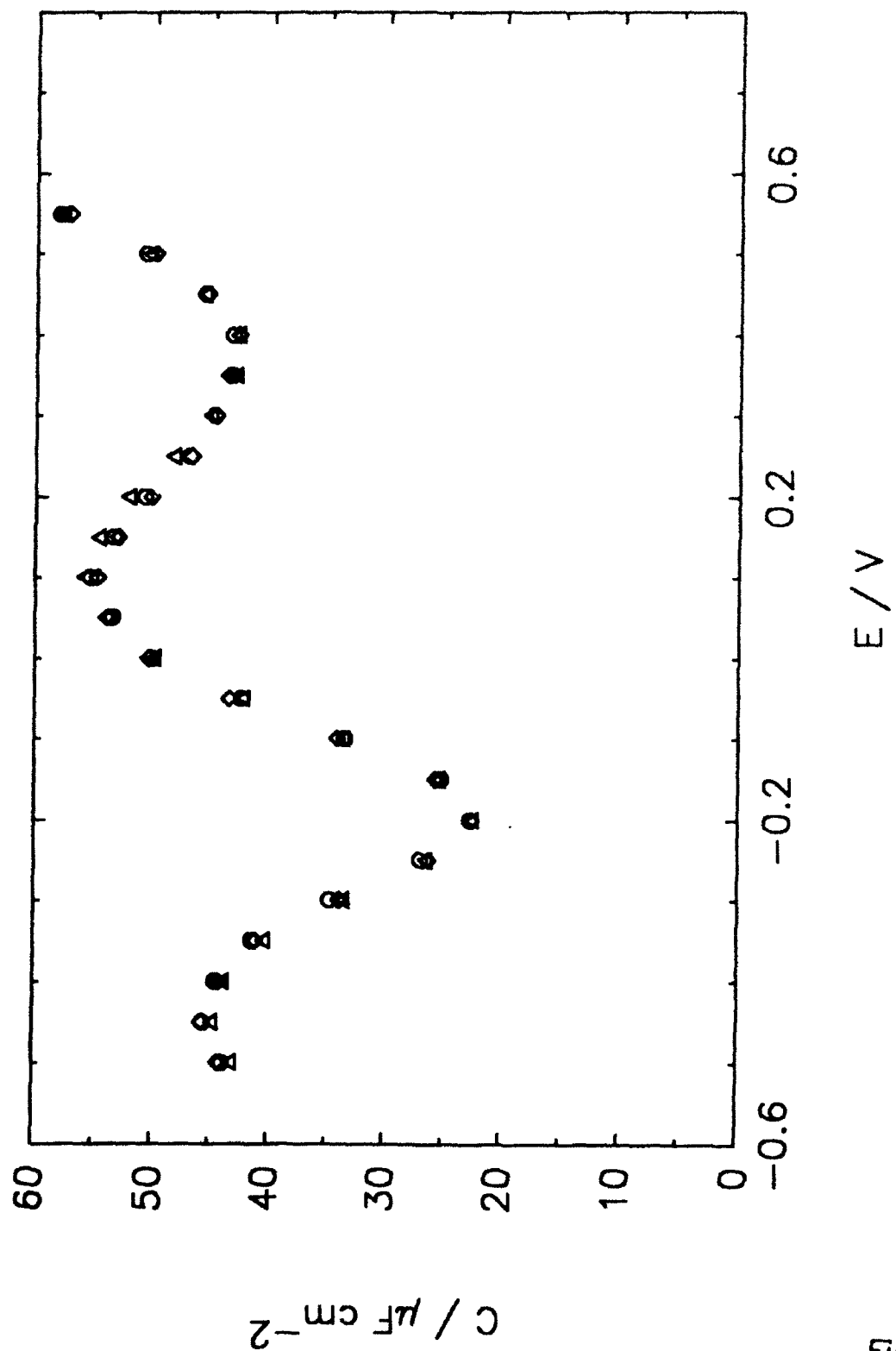


Figure 1

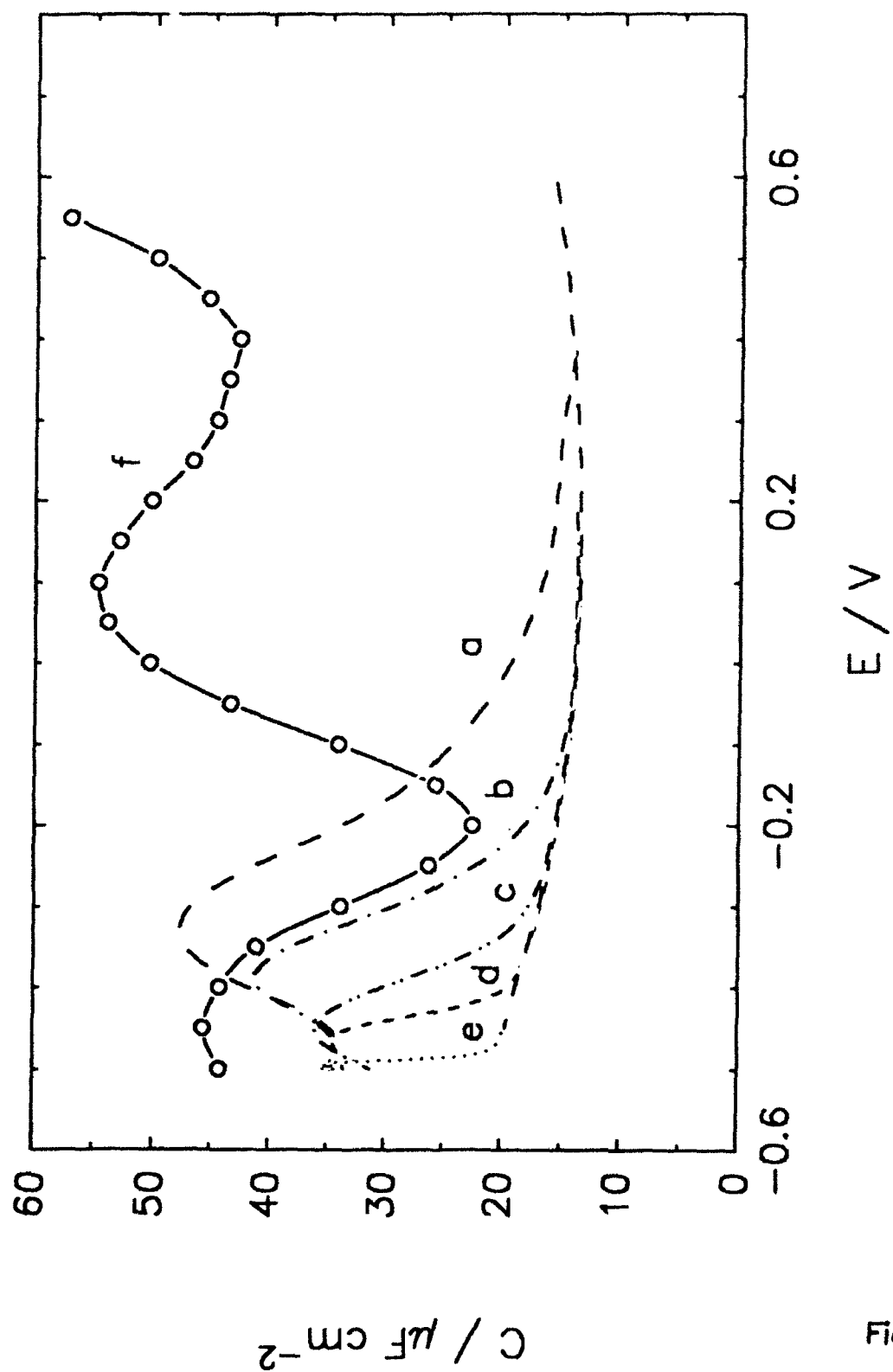


Figure 2



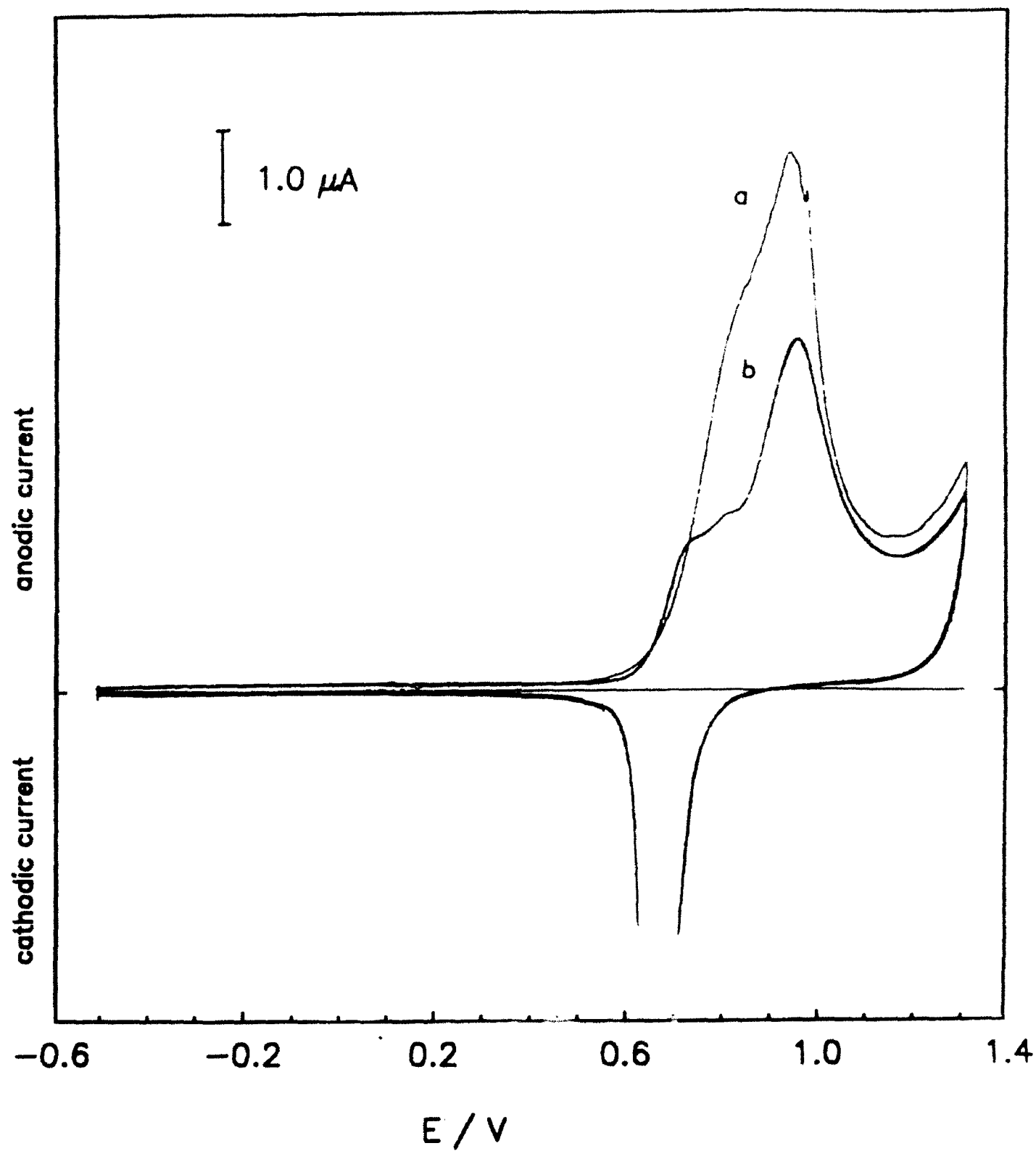


Figure 3

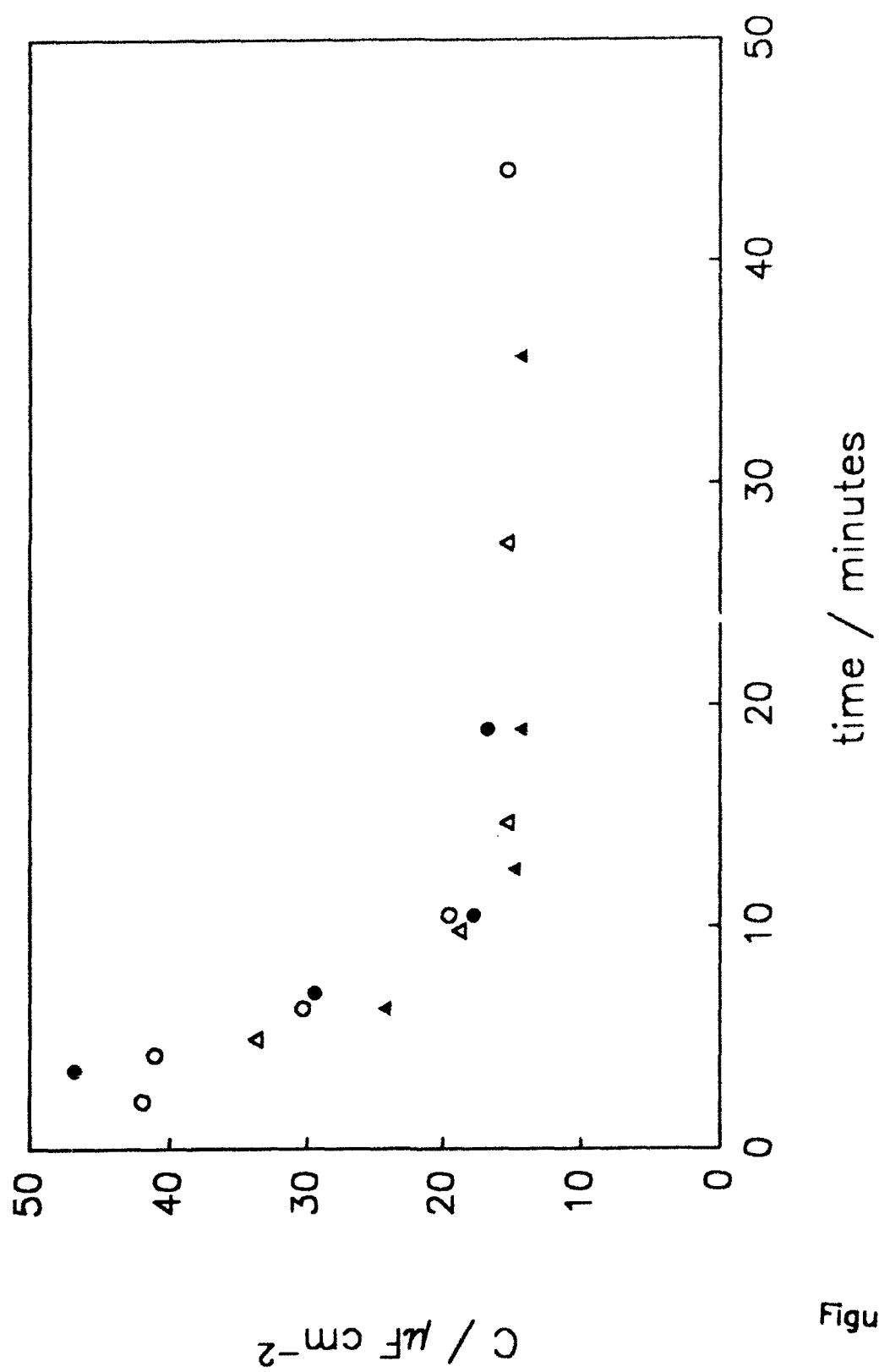


Figure 4

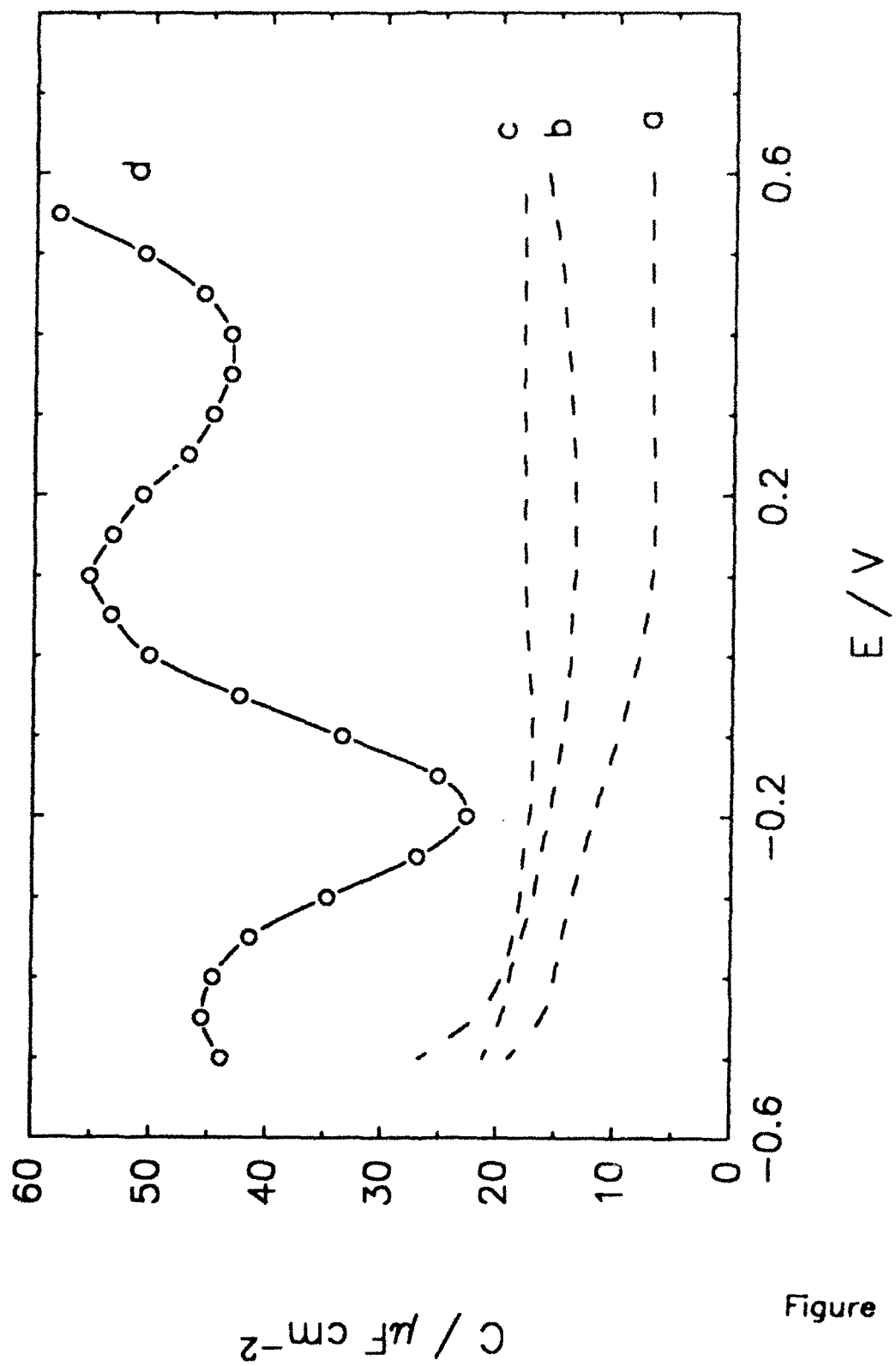


Figure 5

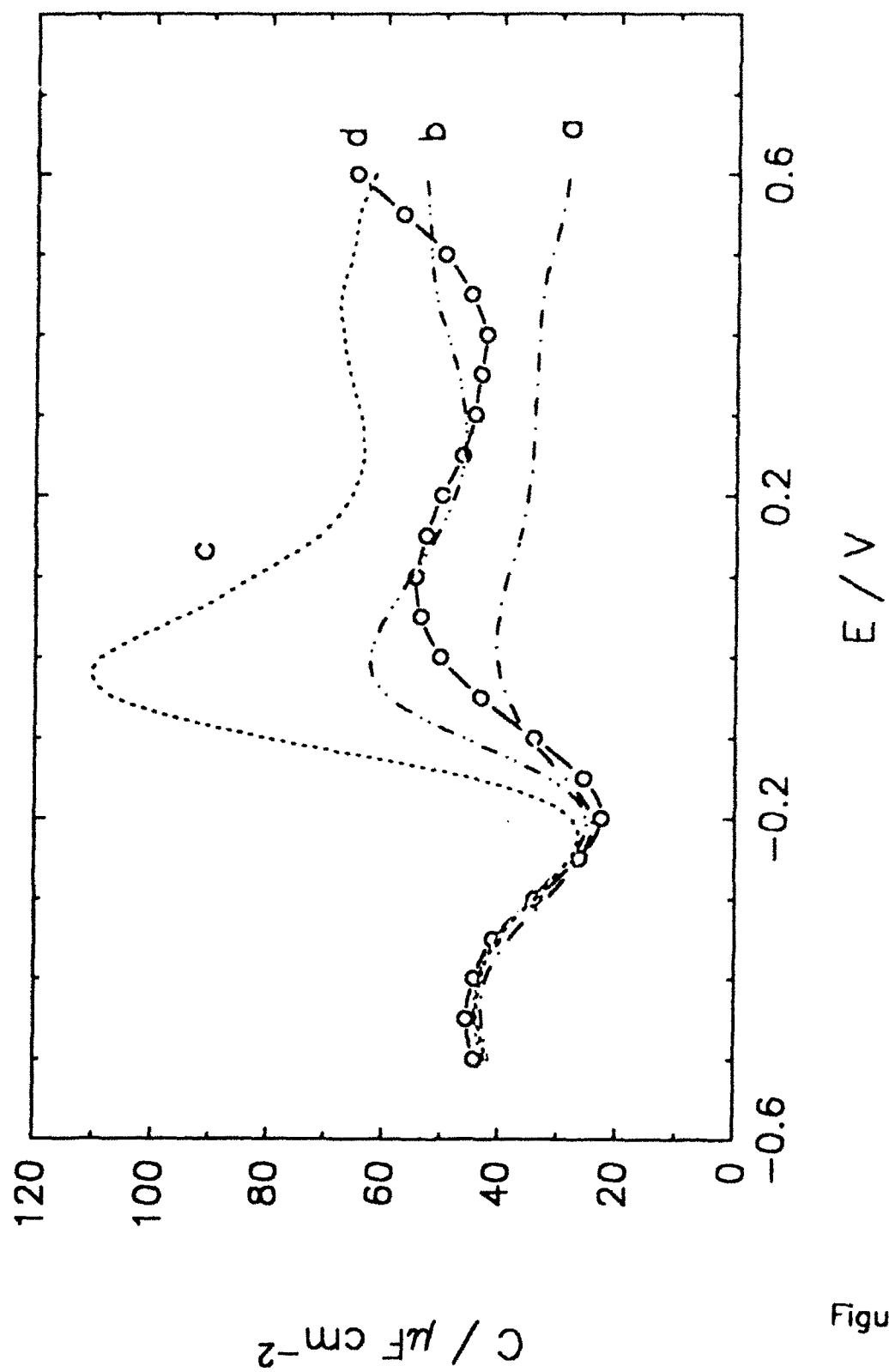


Figure 6

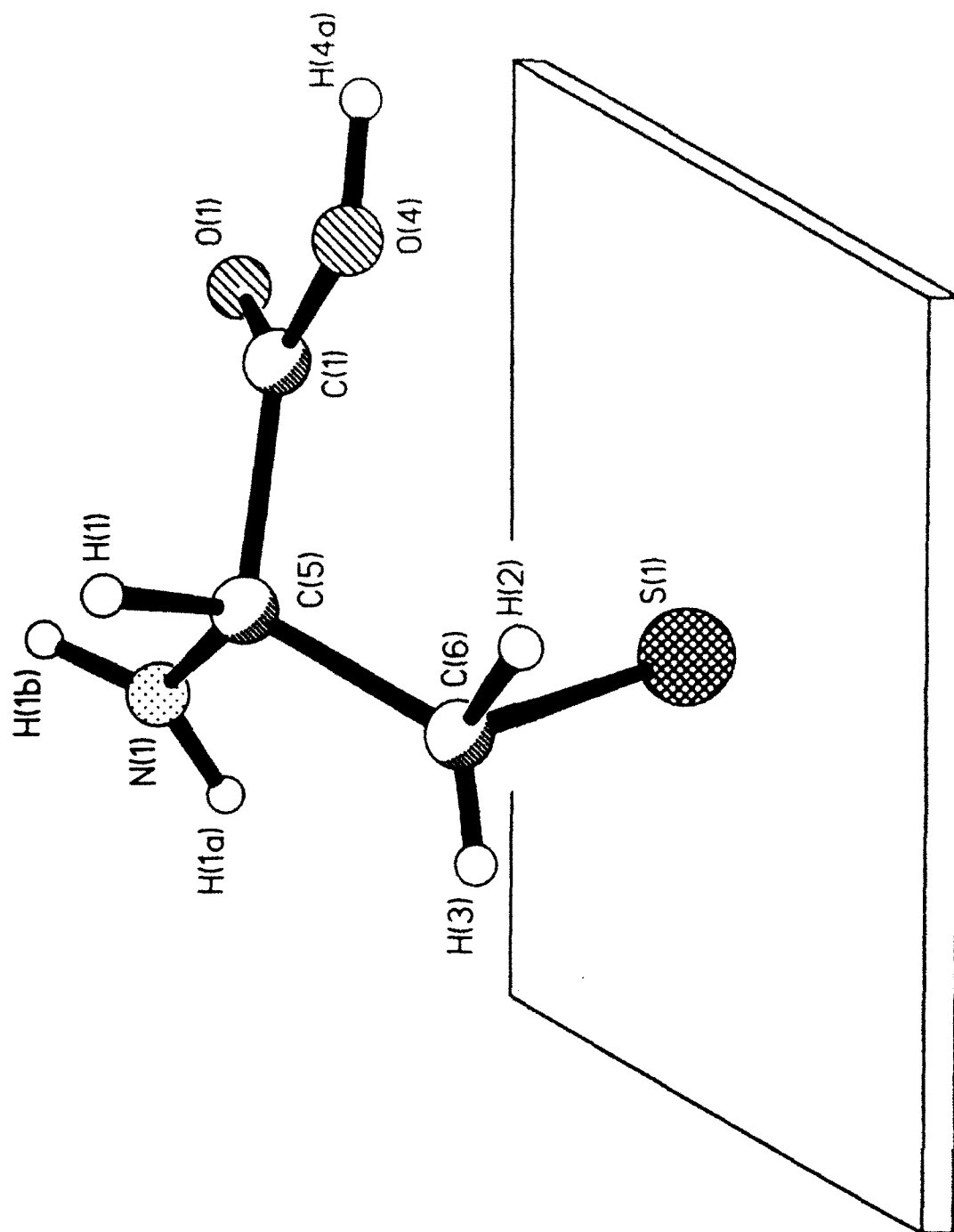


Figure 7